Global Change Biology (2000) **6,** 817–833

CO_2 stabilization, climate change and the terrestrial carbon sink

ANDREW WHITE,* MELVIN G. R. CANNELL* and ANDREW D. FRIEND†
*Institute of Terrestrial Ecology, Bush Estate, Penicuik, Midlothian EH26 0QB, UK; †Center for Environmental Prediction, Rutgers University, 14 College Farm Road, New Brunswick, NJ 08901–8551 at NASA-Goddard Institute for Space Studies, 2880 Broadway, New York, NY 10025, USA

Abstract

A nonequilibrium, dynamic, global vegetation model, Hybrid v4.1, with a subdaily timestep, was driven by increasing CO_2 and transient climate output from the UK Hadley Centre GCM (HadCM2) with simulated daily and interannual variability. Three IPCC emission scenarios were used: (i) IS92a, giving 790 ppm CO_2 by 2100, (ii) CO_2 stabilization at 750 ppm by 2225, and (iii) CO_2 stabilization at 550 ppm by 2150. Land use and future N deposition were not included. In the IS92a scenario, boreal and tropical lands warmed 4.5 °C by 2100 with rainfall decreased in parts of the tropics, where temperatures increased over 6 °C in some years and vapour pressure deficits (VPD) doubled. Stabilization at 750 ppm CO_2 delayed these changes by about 100 years while stabilization at 550 ppm limited the rise in global land surface temperature to 2.5 °C and lessened the appearance of relatively hot, dry areas in the tropics.

Present-day global predictions were 645 PgC in vegetation, 1190 PgC in soils, a mean carbon residence time of 40 years, NPP 47 PgC y^{-1} and NEP (the terrestrial sink) about 1 PgC y^{-1}, distributed at both high and tropical latitudes. With IS92a emissions, the high latitude sink increased to the year 2100, as forest NPP accelerated and forest vegetation carbon stocks increased. The tropics became a source of CO_2 as forest dieback occurred in relatively hot, dry areas in 2060–2080. High VPDs and temperatures reduced NPP in tropical forests, primarily by reducing stomatal conductance and increasing maintenance respiration. Global NEP peaked at 3–4 PgC y^{-1} in 2020–2050 and then decreased abruptly to near zero by 2100 as the tropical source offset the high-latitude sink. The pattern of change in NEP was similar with CO_2 stabilization at 750 ppm, but was delayed by about 100 years and with a less abrupt collapse in global NEP. CO_2 stabilization at 550 ppm prevented sustained tropical forest dieback and enabled recovery to occur in favourable years, while maintaining a similar time course of global NEP as occurred with 750 ppm stabilization. By lessening dieback, stabilization increased the fraction of carbon emissions taken up by the land. Comparable studies and other evidence are discussed: climate-induced tropical forest dieback is considered a plausible risk of following an unmitigated emissions scenario.

Keywords: carbon, climate change, CO_2, ecosystem, sink, tropical forest

Received 20 September 1999; revised version received and accepted 2 March 2000

Introduction

One of the central objectives of the UN Framework Convention on Climate Change is to define a 'safe' future trajectory for atmospheric CO_2 concentrations ([CO_2]) with respect to ecosystems as well as food security and sustainable development. What emissions can be permitted without risking 'dangerous' irreversible change to ecosystems (Parry *et al*. 1996)? This paper makes a contribution to answering this question using the latest

Correspondence and present address: Dr Andrew White, Department of Mathematics, Heriot-Watt University, Edinburgh, EH14 4AS, UK, tel +44/ (0)131 4513222, fax +44/ (0)131 4513249, e-mail a.r.white@hw.ac.uk

output from the UK Hadley Centre Global Climate Model (GCM) transient experiments.

In recent years, increasingly more realistic global ecosystem models have been constructed to determine impacts on ecosystems and the terrestrial carbon balance. However, they will never predict the future with certainty. Uncertainties in the structure and parameterization of these models – revealed, for instance, in recent intercomparisons (VEMAP members 1995; Cramer & Field 1999) – are likely to remain for some time. They can only present possible futures and 'best guesses' of the risks of following given emission scenarios (Hurtt *et al*. 1998). Nevertheless, there are, we suggest, some essential criteria that must be met if models are to make believable assessments of the likely effects of climate change on ecosystems as they will develop over time. These are the assessments required by policy-makers, through the Intergovernmental Panel on Climate Change.

First, they must be 'dynamic global vegetation models' (DGVMs), combining (i) coupled plant-soil carbon, N (biogeochemical) and water cycles, (ii) atmosphere-vegetation energy and mass (biophysical) transfers, and (iii) dynamic (biogeographical) shifts in vegetation types, structure and properties, simulating spatially explicit changes in biomes around the world. There are few models of this kind (Foley *et al*. 1996; Friend *et al*. 1997; see Neilson & Running 1996; Hurtt *et al*. 1998; Neilson *et al*. 1998). Secondly, they must have transient, time-evolving behaviour. Most models simulate equilibrium conditions in given climates and move from one equilibrium to another in single steps (Schimel *et al*. 1997a; Parton *et al*. 1995; McGuire *et al*. 1997; Xiao *et al*. 1997). Non-equilibrium models are still rare (Foley *et al*. 1996; Friend *et al*. 1997). Thirdly, the ecosystem models must be driven using transient climate predictions with realistic interdecadal and interannual variability. These climate data have only recently become available for different CO_2 emission scenarios but daily and inter-annual variability must still be generated from annual or decadal means from the GCMs. It is clear, however, that transient climates can produce very different vegetation responses compared with equilibrium climates, even using equilibrium ecosystem models (e.g. Cao & Woodward 1998; Neilson & Drapek 1998; Xiao *et al*. 1998). Fourthly, consideration should be given to: (i) spatial patterns of land use, although Kicklighter *et al*. (1999a) concluded that differences in model performance were due more to conceptualization that to differences in representation of land use, and (ii) the impact of future atmospheric N deposition (Hudson *et al*. 1994; Townsend *et al*. 1996; Holland *et al*. 1997), although this is difficult as long as there are large uncertainties about the fate of this N (Houghton *et al*. 1998; Nadelhoffer *et al*. 1999). Lastly, ecosystem models should be fully coupled to GCMs to capture the potentially important feedbacks between land-surface properties, climate and the concentration of greenhouse gases in the atmosphere (e.g. Lean *et al*. 1996; see Hurtt *et al*. 1998).

This paper reports predictions of terrestrial carbon stocks, net primary productivity (NPP) and net ecosystem productivity (NEP) made using Hybrid v4.1 (Friend *et al*. 1997), a DGVM constructed to meet the first two criteria listed above. Hybrid was the only nonequilibrium model in the Potsdam intercomparison of 17 models (Cramer & Field 1999). This study meets the third criterion by using transient climate predictions made by the UK Hadley Centre GCM (HadCM2) with different IPCC atmospheric CO_2 stabilization scenarios. Decadal mean monthly climate output was converted to variable daily, seasonal and annual climate and weather using a stochastic weather generator (Friend 1998). The fourth criterion, to include land use and N deposition, was not met in this study and Hybrid was not coupled with the GCM. Nevertheless, this study offers a significant advance on previous studies and, unlike other studies of its kind, identifies potentially damaging effects of climate change on tropical forests and possible benefits of CO_2 stabilization.

Materials and methods

Dynamic Global Vegetation Model, Hybrid v4.1

The Hybrid v4.1 ecosystem model is not described in detail here, because a complete description is given by Friend *et al*. (1997) (see also Friend 1995). The model is described further by (i) Friend & White (2000), who evaluated its ability to simulate measured carbon fluxes at particular sites and the preindustrial global distribution of vegetation types, NPP and carbon standing stocks, and also (ii) Cannell *et al*. (1998) and White *et al*. (2000), who used the model to examine effects of climate change on UK forests and the northern terrestrial carbon sink, respectively. In the Potsdam NPP model intercomparison, Hybrid was shown to simulate observed spatial and temporal patterns of global NPP, its components (absorbed photosynthetically active radiation and light use efficiency) and estimated latitudinal trends in $[CO_2]$ seasonal amplitude, which compared favourably with observations and other models, taking into account that Hybrid was run at preindustrial CO_2 concentrations (Cramer & Field 1999).

The model combines biogeochemical, biophysical and biogeographical processes in the soil–plant–atmosphere system. The carbon, water and nitrogen cycles are coupled, including all the major interactions, feedbacks and exchanges between the soil, vegetation and atmosphere. All underlying processes are calculated on a day-

and night-time step. The model has true transient behaviour by simulating annual growth and competition among plant types. The model simulates potential vegetation but does not, in this application, include land use or natural disturbance.

The model is parameterized for three main classes of vegetation: herbaceous, broadleaved trees and needle-leaved trees, which are given different values of up to 16 parameters (see Tables 1 and 2 of White *et al*. 2000). These main classes are then divided into eight generalized plant types by distinguishing C3 and C4 herbaceous plants, evergreen and deciduous trees and cold and dry deciduous trees. C3 and C4 herbaceous plants have different photosynthesis submodels; cold deciduous trees shed their leaves in response to daylength and refoliate in response to a degree-day requirement; dry deciduous trees shed their leaves when the soil water potential falls below –1.49 MPa and refoliate when it rises above –0.5 MPa (Friend & White 2000).

The model operates conceptually like a forest gap model (Shugart 1984), with 200 m^2 plots in which individuals can grow, die and regenerate year by year. The parameter values of the eight plant types determine their success in competing for light, water and N in any climate and hence the resulting vegetation. Thus, unlike most gap models, plant growth in Hybrid is determined entirely by [CO_2], N inputs and climatic variables operating through plant physiological and soil processes rather than empirical functions. Initial soil carbon content is derived from an observed relationship between soil carbon and current precipitation and temperature (Friend & White 2000). Initializing soil carbon in this manner speeds up the convergence towards near equilibrium (where litter inputs from vegetation balance soil respiration losses) during an initial 500-y run under current conditions. At the end of this initial run vegetation carbon is also near equilibrium (NPP is in balance with litter losses) and can be composed of different proportions of eight plant types. Thereafter the model simulates transient changes in vegetation properties and soil–vegetation carbon stocks as climate and [CO_2] change.

C3 and C4 photosynthesis are calculated using a biochemical approach based on Farquhar & von Caemmerer (1982) and Collatz *et al*. (1991), respectively. Canopy photosynthesis is related linearly to the photosynthetic rate of the uppermost leaves with the vertical profile of N in the canopy optimized to time-averaged profiles of photosynthetically active radiation. Stomatal conductance is calculated using empirical relationships from Jarvis (1976) adapted by Stewart (1988) (see Appendix). Maintenance respiration is calculated as described in the Appendix. Allocation is based on allometric relationships and fixed ratios, such as foliage to sapwood area and foliage to fine root mass. Dynamic equations define processes such as root N uptake, C and N storage, foliage senescence, phenology and sapwood–heartwood conversion, modulated by temperature and/or water and N status. Day and night energy balances of the soil and canopy are solved to calculate rates of soil evaporation, evaporation of intercepted precipitation, rates of transpiration and foliage temperature.

Soil C and N dynamics are based on Century (Parton *et al*. 1993) as formulated by Comins & McMurtrie (1993). The soil is divided into three layers: 0–5 cm, 5–20 cm and 20–100 cm depth. Herbaceous vegetation has access to water and N in the top two layers, whereas trees can access all layers. The total soil-water holding capacity is determined from soil carbon and soil-water potentials are calculated (Friend *et al*. 1997). A soil temperature profile is used to calculate the depth of frozen soil at high latitudes, with all water below this depth assumed frozen, and therefore unavailable and forming an increased resistance to drainage (Wang & Polglase 1995; White *et al*. 2000).

Runs of the Global Climate Model and DGVM (Hybrid v4.1)

The Hybrid model was driven using transient climate output from the UK Hadley Centre coupled atmosphere–ocean GCM (HadCM2), supplied as decadal monthly means with predicted levels of interdecadal variability. There was no *a priori* assumption that the climate will become more variable. This GCM was run with a climate sensitivity of about 2.5 °C equilibrium global warming at double preindustrial [CO_2] during the first 100–200 y of integration. The mean output was taken of four ensemble runs to 2100 with the IPCC Scenario1992a of increasing [CO_2] (IS92a, equal to an increase of 1% per year) to give the IS92a scenario. The two stabilization scenarios were derived from output to 2250 with [CO_2] stabilizing at 750 ppm by 2225 or 550 ppm by 2150, following IPCC trajectories (Schimel *et al*. 1995) (Fig. 1a). Concentrations of other greenhouse gases and aerosols were held constant at 1990 values. Global carbon emissions in the IS92a, 750 ppm and 550 ppm scenarios from 1990 to 2100 were about 1500, 1230 and 920 PgC, respectively. Climate predictions from the four IS92a runs produced different patterns of interdecadal climate variability, but similar time trends and global spatial patterns of climate. These have been shown, in a separate study, to generate similar patterns of change in terrestrial carbon (White *et al*. 1999).

The GCM predictions closely matched observed temporal and spatial pattern of climate since preindustrial times (Mitchell *et al*. 1995; Johns *et al*. 1997). However, as with most GCMs, absolute predictions of future climates were considered to be less reliable than

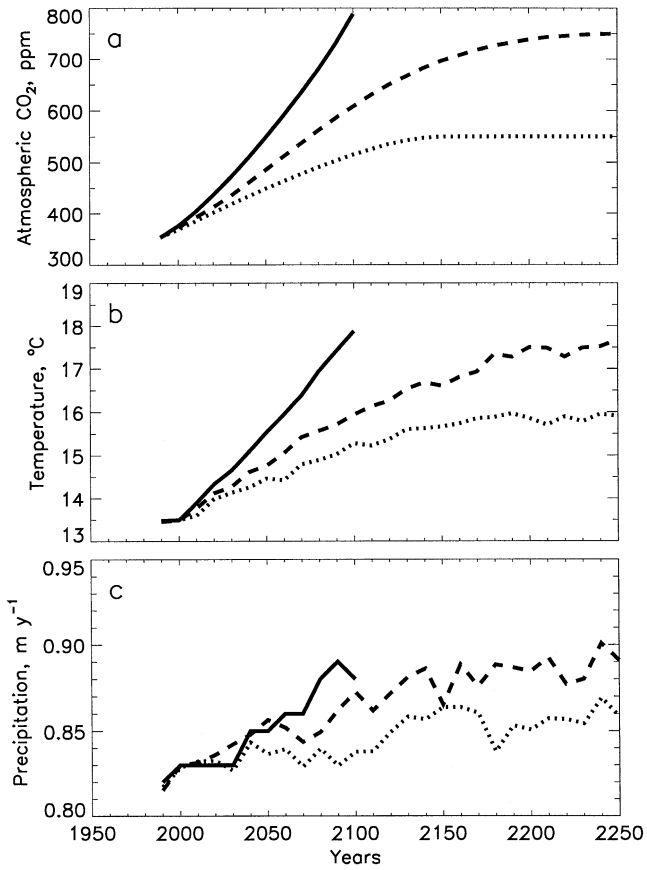

Fig. 1 (a) Prescribed trajectories of atmospheric CO_2 concentrations ($[CO_2]$) used for both the GCM and DGVM: solid line, IPCC Scenario 1992a (IS92a); dashed line, stabilization at 750 ppm $[CO_2]$; dotted line, stabilization at 550 ppm $[CO_2]$ (Schimel *et al*. 1995). (b) and (c) Corresponding predicted mean decadal global land-surface temperature and precipitation, according to the UK Meteorological Office GCM (HadCM2).

climate anomalies (Ciret & Henderson-Sellers 1997). Consequently, GCM anomalies of temperature, diurnal temperature range, relative humidity, downward shortwave radiation and precipitation were calculated as mean decadal monthly differences relative to the GCM predictions for the 1990s. These anomalies were then added to a global observed climatology for 1961–90 (Hulme *et al*. 1999; New *et al*. 1999) which was re-gridded to the GCM scale (2.5-3.75°; latitude-longitude). Annual, seasonal, daily, daytime and night-time values of the climate variables, required by Hybrid, were then derived from the decadal monthly means using a stochastic weather generator parameterized for each decade (Richardson & Wright 1984; Friend 1998).

The Hybrid model was run for 500 y to reach a near steady-state in the observed global climate (Hulme *et al*. 1999). It was then run with each of the three transient climates starting in 1990; thus the 1990s decade was the first in which transient change was simulated. Ten independent 200 m^2 plots were used in each GCM grid square to obtain reliable mean ecosystem behaviour (Friend *et al*. 1997; Friend & White 2000).

Biological N_2 fixation was assumed to be 10 kg N ha^{-1} y^{-1} everywhere (cf. Cleveland *et al*. 1999) and atmospheric N deposition for each grid square was derived from NH_x and NO_y deposition estimates for the 1990s (Holland *et al*. 1997; Dentener, pers. comm.). In this analysis, N deposition was kept constant throughout the simulations.

Results

Climate predictions

In the IS92a scenario, the global mean annual temperature of the land surface (excluding Antarctica) was predicted to increase from 13.5 °C in 1990 to 17.8 °C in 2100 (Fig. 1b) a rise of 4.3 °C (0.4 °C per decade). This was greater than the global average (3.4 °C from 1990 to 2100 with HadCM2 and IS92a) because warming was less over the oceans. It is important to note that warming was greatest in both tropical and boreal regions and that some tropical *land* areas were predicted to warm by over 4.5 °C by 2100, equally as much as northern high-latitude lands (Fig. 2a).

Global mean warming predicted by the Hadley Centre GCM is within the range predicted by other major GCMs (Kattenberg *et al*. 1996; Neilson & Drapek 1998; their table 2) but is greater than, for instance, the 2.1 °C warming predicted by 2100 with IS92a emissions by

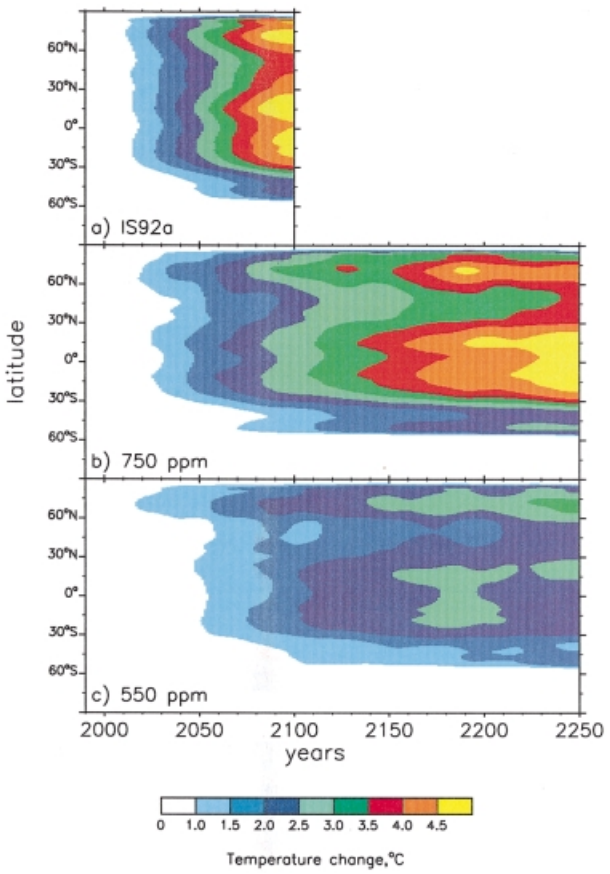

Fig. 2 Predicted changes in land-surface latitudinal temperature relative to the 1990s (taken as the mean 1960–90 observed climatology). Predictions are shown for (a) IS92a, (b) 750, and (c) 550 ppm [CO_2] stabilizations, according to HadCM2.

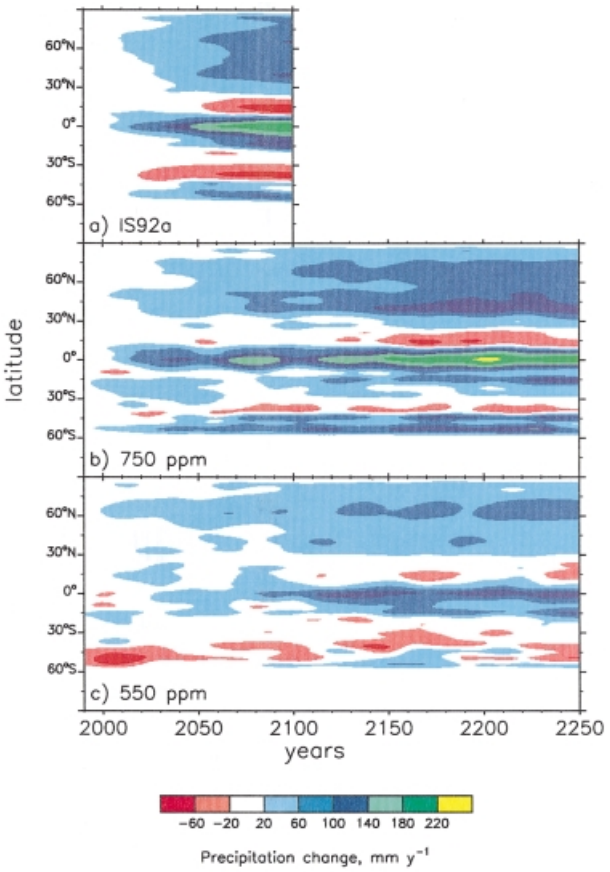

Fig. 3 Predicted changes in land-surface latitudinal precipitation relative to the 1990s (taken as the mean 1960–90 observed climatology). Predictions are shown for (a) IS92a, (b) 750, and (c) 550 ppm [CO_2] stabilizations, according to HadCM2.

Schimel *et al*. (1997b) using a simpler GCM, and is much greater than the 0.25 °C warming per decade predicted by the Integrated Global System Model with similar transient CO_2 forcing (Xiao *et al*. 1998; see Fig. 9).

Stabilization at 750 ppm [CO_2] slowed the mean rate of global land warming to about 0.21 °C per decade from 1990 to 2100, with warming stabilizing at about 4 °C by 2200 (Fig. 1b). Again, warming was greatest in both boreal and tropical regions, with a distinct lag in warming at northern temperate latitudes (Fig. 2b). Stabilization at 550 ppm [CO_2] by 2150 slowed the mean rate of warming to about 0.15 °C per decade between 1990 and 2100 and warming stabilized at about 2.5 °C by 2190, with only the boreal region warming by more than 3.0 °C (Fig. 2c).

Global mean precipitation over the land surface was predicted to increase from about 0.82–0.89 m y^{-1} between 1990 and 2100 in the IS92a scenario – an increase of 8.5% (Fig. 1c). Stabilization at 750 ppm [CO_2] delayed this increase in rainfall by about 50 y. Stabilization at 550 ppm [CO_2] prevented global rainfall from increasing more than about 5%. However, these global means disguise important latitudinal variation. In all scenarios, there were marked decreases in rainfall in some tropical regions at about latitudes 20 °N (especially in northern S. America) and 40 °S (including Australia) (Fig. 3). Rainfall increases were greatest in the equatorial tropics and at northern temperate and boreal latitudes (Fig. 3).

Climate changes in the tropics were especially important in this study. Hulme & Viner (1998) presented a comprehensive analysis of predictions of one of the HadCM2 IS92a transient experiments used in this study. Rainfall was predicted to decrease over much of the Amazon basin, southern and western Africa and central and western Australia, with a clear tendency for dry seasons to become longer and more severe, with greater interannual variability in rainfall. Throughout much of the tropics, soil moisture levels declined, especially in northern South America.

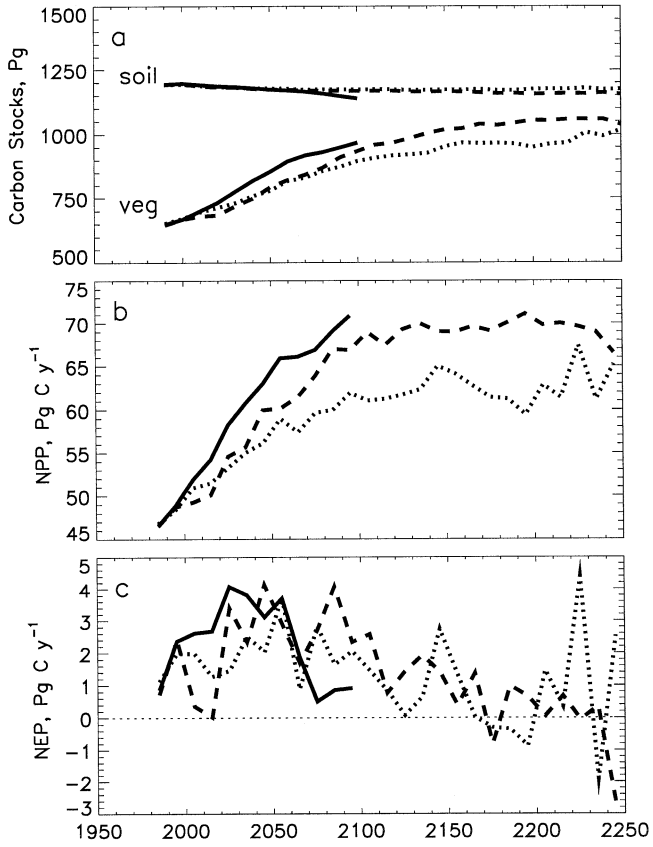

Fig. 4 (a) Global stocks of carbon in vegetation and soils (b) global annual net primary productivity (NPP), and (c) global net ecosystem productivity (NEP), predicted using the Hybrid model in response to climate change and increasing [CO_2] with IS92a forcing (solid line), stabilization at 750 ppm [CO_2] (dashed line), and stabilization at 550 ppm [CO_2] (dotted line). Values shown are decadal means.

Predicted carbon stocks, net primary productivity (NPP) and net ecosystem productivity (NEP)

Present-day vegetation was predicted to contain 645 PgC and soils 1190 PgC (Fig. 4a) – both within the range of global inventory estimates of 420–830 PgC in vegetation and 1100–1600 PgC in soils (Post *et al*. 1982, 1997). In all scenarios, global vegetation carbon increased by 45–50% over the simulation period, while soil carbon decreased by less than 5% (Fig. 4a) with no marked latitudinal difference. Slowing the rate of increase in [CO_2] slowed the rate of increase in vegetation carbon, because the CO_2-fertilization effects were diminished, and decreased the small loss in soil carbon, because temperatures rose more slowly.

Present-day global NPP was 47 PgC y^{-1} (Fig. 4b) and was predicted to increase substantially in all [CO_2] scenarios – for instance, by 45, 39 and 29% between 1990 and 2100 in the IS92a, 750 and 550 ppm [CO_2] scenarios, respectively (Fig. 4b). The global trajectories of increase in NPP were similar to the trajectories of increase in [CO_2], but with interannual variability due to the generated climatic variation (Figs 4b and 1a). Most importantly, NPP increased markedly at northern latitudes (30–65 °N, especially at 45–60 °N) and decreased at equatorial latitudes (Fig. 5). The latter was visually correlated temporally and spatially most closely with temperatures and vapour pressure deficits, and to a lesser extent rainfall. NPP decreased at equatorial latitudes in the IS92a and 750 ppm [CO_2] scenarios when warming exceeded about 3.5 °C (Figs 5 and 2) and VPDs increased by over 80%.

In Hybrid, the mean carbon residence time in 1990, calculated as the annual mean total carbon stock divided by annual heterotrophic respiration (R_h), was about 40 years globally, varying from 25 years in the tropics to 63 years at latitudes above 50 °N. In other words, the increase in R_h lagged behind the increase in NPP causing an increase in NEP – i.e. creating a carbon sink (Friedlingstein *et al*. 1995; Lloyd & Farquhar 1996).

NEP was highly variable, spatially and temporally, being a small difference between two large variable quantities, NPP and R_h. (Figs 4c and 6). At any location NEP often changed sign from year to year due to climate variability and the stochastic nature of the model. Nevertheless, there were clear global and regional trends.

Current global NEP was estimated to be about 1 PgC y^{-1} (Fig. 4c). Positive NEP values were predicted at both northern temperate–boreal and tropical latitudes. The global sink was predicted to increase, peaking at 3–4 PgC y^{-1} in the period 2020–2050 (somewhat earlier in

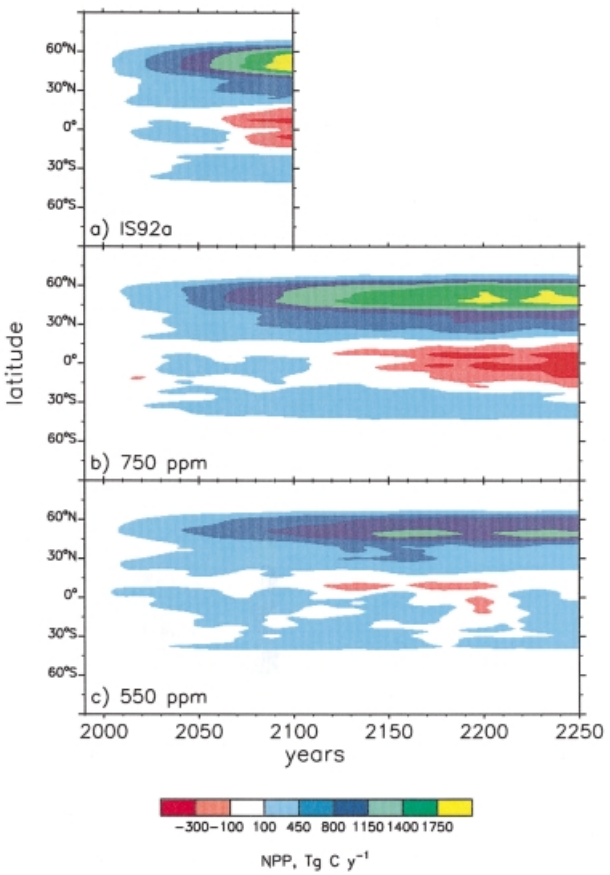

Fig. 5 Predicted change in latitudinal net primary productivity (NPP) relative to the 1990s. Predictions are made using the Hybrid model in response to climate change and increasing [CO_2] with (a) IS92a forcing, (b) stabilization at 750 ppm [CO_2], and (c) stabilization at 550 ppm [CO_2]. Values shown are interpolated decadal means. Note that values are given in Tg per one degree of latitude and so are biased by the latitudinal distribution of land area.

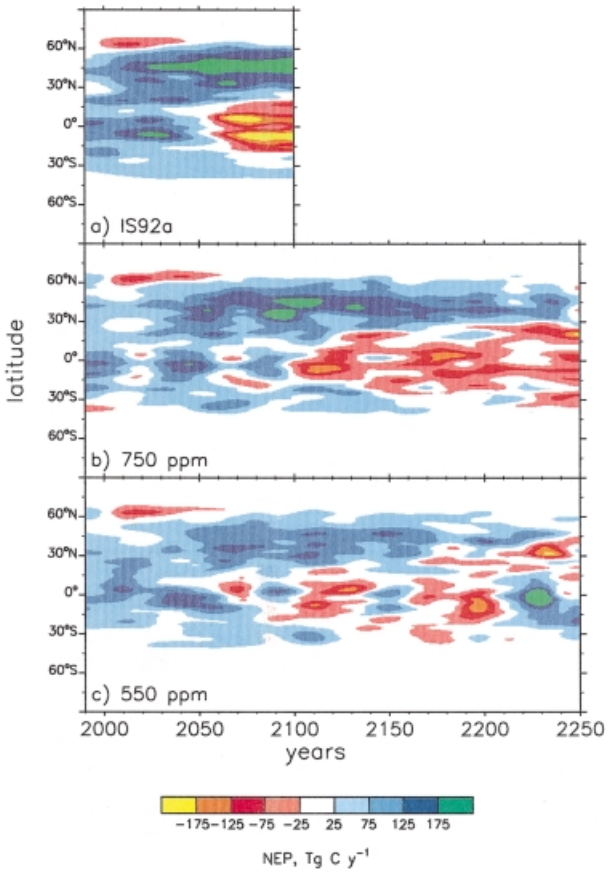

Fig. 6 Predicted change in latitudinal net ecosystem productivity (NEP) relative to the 1990s. Predictions are made using the Hybrid model in response to climate change and increasing [CO_2] with (a) IS92a forcing, (b) stabilization at 750 ppm [CO_2], and (c) stabilization at 550 ppm [CO_2]. Values shown are interpolated decadal means. Note that values are given in Tg per one degree of latitude and so are biased by the latitudinal distribution of land area.

the higher [CO_2] scenarios) and then decrease to fluctuate around zero by around 2175. In the IS92a scenario, the decrease occurred precipitously in the 2060–2080 period owing to a large loss of carbon from tropical regions associated with forest dieback (see below). Consequently, the global carbon sink virtually disappeared despite a continuing strong sink at mid-high northern latitudes (Figs 4c and 6a). In the 750 and 550 ppm [CO_2] stabilization scenarios, the global sink weakened more gradually (after NPP stabilized) and settled to around zero after 2150. Thus, both of these stabilization scenarios delayed the disappearance of the terrestrial carbon sink by about 100 y.

However, the global average responses of the two stabilization scenarios were similar for different reasons. In the 750 ppm [CO_2] stabilization scenario, there was substantial loss of carbon in some years in the tropics after about 2100, while the northern sink persisted to at least 2200 (Fig. 6b). This caused variation in NEP and the eventual loss of the terrestrial carbon sink. By contrast, in the 550 ppm [CO_2] scenario the atmospheric CO_2 concentration stabilizes in 2150, and hence the depletion of the sink after this period occurs as the biosphere and climate relax to a new equilibrium. In some tropical regions, this new climate equilibrium is close to the threshold which produces tropical forest dieback (see later, Fig. 8) and here the decadal variability in climate causes the tropics to switch more readily between carbon source and sink causing global variability in NEP from 2150 onwards. The northern sink was smaller and decreased to near zero by 2200 (Fig. 6c).

The prediction of carbon release to the atmosphere as a result of tropical forest dieback negated some of the benefit of CO_2 fertilization in the high-emission scenar-

ios. Consequently, the terrestrial sink absorbed the smallest fraction of emitted carbon in scenarios with most dieback. Between 1990 and 2100, global terrestrial carbon uptake in the IS92a, 750 and 500 ppm [CO_2] stabilization scenarios was 265, 263 and 223 PgC, representing 18, 21 and 24% of 1990–2100 emissions (1500, 1230 and 920 PgC), respectively.

Carbon gain at northern latitudes and loss in the tropics

The strong sink at northern temperate-boreal latitudes was the result of an increase in the biomass of forests which already existed in 1990 (NPP exceeded R_h) plus some expansion in forest area, as described for the boreal region for the IS92a scenario by White *et al*. (2000). A short-lived source of carbon occurred at about 60 °N between the years 2020 and 2050 when increased R_h owing to warming exceeded the increase in NPP due to CO_2 fertilization (White *et al*. 2000).

The carbon source in the tropics was due to forest dieback which resulted from NPP reductions due to climate-driven stomatal closure and increased plant maintenance respiration. Thus, R_h exceeded NPP and produced negative NEP values (Fig. 6). This occurred in northern S. America, southern equatorial Africa and to a lesser extent in south-east Asia (Fig. 7). In these areas, tropical forests were replaced by savanna, grassland and even desert once decadal mean temperatures rose about 4 °C above the 1961–90 average, reaching 31–33 °C. Closer examination showed that, at the time of dieback, these areas experienced temperature increases of over 6 °C in some years and more in some months. More importantly, simultaneous decreases in rainfall and prolonged, more severe dry seasons were associated with large increases in vapour pressure deficit (VPD). This is illustrated in Fig. 8 for a region in northern South America where biomass decreased to zero in the IS92a and 750 ppm [CO_2] stabilization scenarios when decadal mean annual temperatures rose to 31 °C, rainfall decreased by over 10%, from about 2.1 to 1.8 m y^{-1}, and annual mean VPD doubled.

In regions of dieback, high temperatures and plant water stress decreased gross primary production (GPP) and increased plant respiration resulting in a negative carbon balance and eventual tree death. The two crucial assumptions in the Hybrid model which produced this negative balance were (i) decreased stomatal conductance in response to increased VPD, formulated as a linear increase in a stress factor to a threshold value, and (ii) an exponential increase in maintenance respiration with increase in temperature. (The equations and parameters used are described in the Appendix.)

Stabilization at 550 ppm [CO_2] prevented prolonged periods occurring in the tropics when high temperatures, low rainfall and high VPD produced conditions critical for the survival of tropical forests. There were some years when VPDs were high and forests died in the model (e.g. about 2200 in Fig. 8) resulting in negative NEP (Fig. 6c), but the forests were able to regrow subsequently when conditions became more favourable (e.g. after 2200 in Fig. 8 and about 2150 and 2230 in Fig. 6c). In short, 550 ppm [CO_2] stabilization did not avoid forest dieback (within the Hybrid model), but it did prevent widespread irreversible loss of forest, suggesting that it was close to the threshold of a 'safe' [CO_2] trajectory.

Discussion

The predictions presented here are made using transient climate output from a state-of-the art GCM and a DGVM with transient behaviour which combines biogeographical, biophysical and biogeochemical processes. The results therefore provide one of the first DGVM estimates of the time-dependent behaviour of the terrestrial carbon sink in response to plausible scenarios of developing climate change. The predictions are, nevertheless, from only one GCM and DGVM and so present one set of possible futures, none of which should be regarded as forecasts. Also, it is important to remember that this study did not include land-use change, natural disturbance by fire and other agents, future N deposition, limitations imposed by phosphorus and other nutrients, and the ecosystem model was not coupled with the GCM and so had no feedback effects on climate or [CO_2]. In reality, differences in terrestrial carbon uptake could modify atmospheric CO_2 trajectories by up to 15% and hence effect predictions of climate change (Lenton 2000).

Nevertheless, the possible futures predicted in this study contribute new information on (i) the current magnitude and whereabouts of the terrestrial carbon sink, (ii) its future development in response to different levels of climate change, (iii) the possible increase in the high latitude terrestrial carbon sink, and (iv) the vulnerability of tropical carbon sink. Each of these topics is discussed below, comparing the results of this study with previous published work.

Magnitude of the global terrestrial carbon sink

An unforced outcome of increasing [CO_2] in the Hybrid model (i.e. without calibration or tuning) was the prediction of a current global terrestrial carbon sink of about 1 Pg C y^{-1} (Fig. 4c). This is within the range of estimates made by deconvolution of the historic [CO_2] record, which generate a net terrestrial flux to balance the record with known industrial emissions, modelled

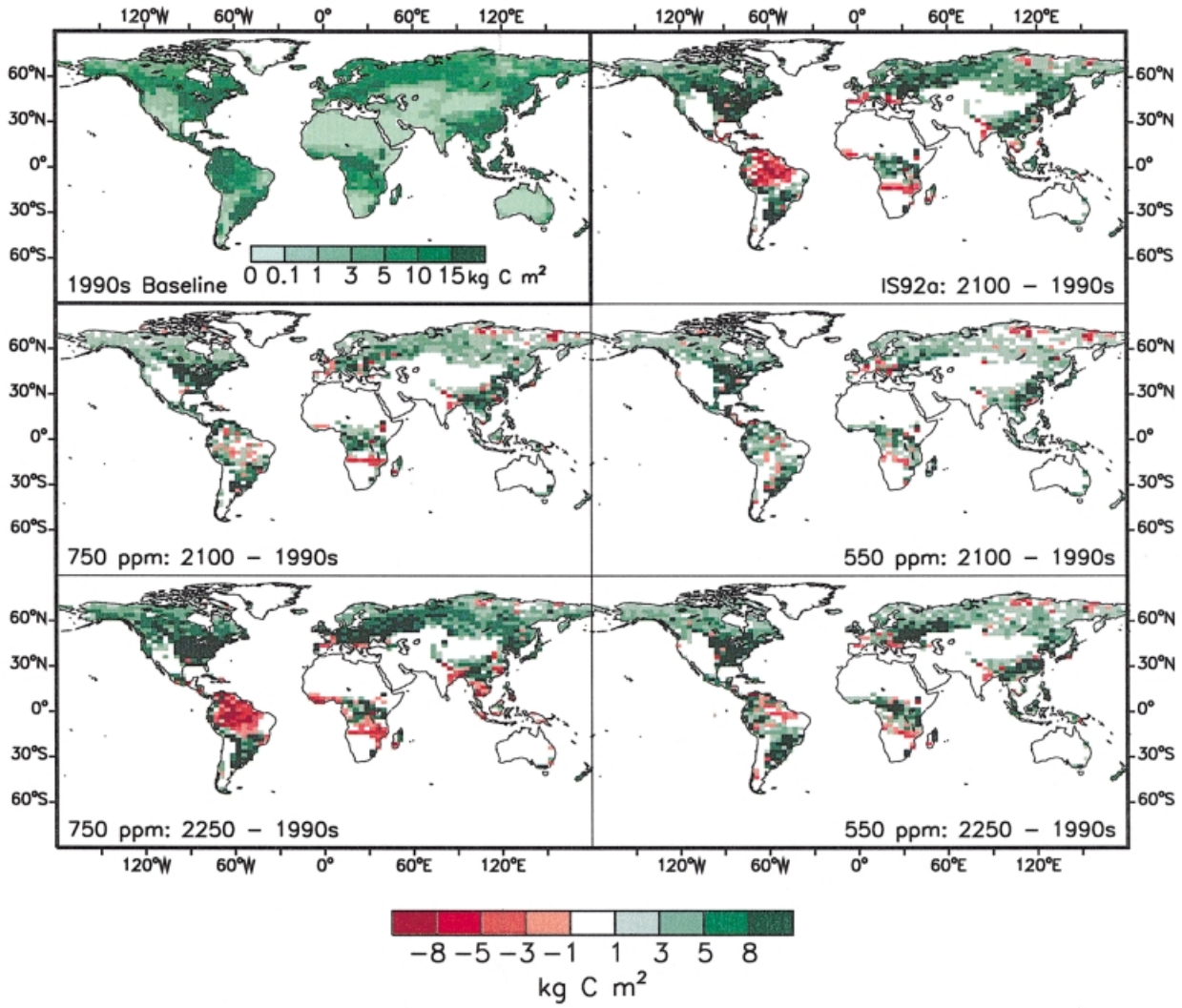

Fig. 7 Global vegetation biomass ($kg\,C\,m^{-2}$) in the 1990s and the change in biomass between the 1990s and 2100 in response to climate change and increasing [CO_2] with IS92a forcing, 750 ppm and 550 ppm [CO_2] stabilization, and between the 1990s and 2250 for the two stabilization scenarios.

oceanic uptake and estimated land-use emissions (Bruno & Joos 1997; Post *et al*. 1997).

The model also predicted interannual variability in the global sink exceeding $-1\,PgC\,y^{-1}$ as a result of variation in decadal, annual and seasonal weather, causing changes in annual NPP and in the time-lag between changes in NPP and R_h (note that Fig. 4c gives decadal means). Equally large interannual variation is predicted in atmospheric CO_2 inversion studies (e.g. Keeling *et al*. 1995), deconvolution studies of the historic [CO_2] record (e.g. Post *et al*. 1997), other ecosystem modelling studies (Kaduk & Heimann 1994; Kinderman *et al*. 1996; Schimel *et al*. 1996; Xiao *et al*. 1998) and is implied in the large year-to-year variation in satellite vegetation index (Potter & Klooster 1999) and measured net CO_2 fluxes over vegetation (Chen *et al*. 1999; Malhi *et al*. 1999). Such large variation makes it almost impossible to estimate trends in the terrestrial carbon sink by means other than modelling.

It is well-recognized that the size of the terrestrial carbon sink at any time depends on (i) the magnitude of NPP, (ii) the rate at which NPP is increasing, and (iii) the turnover time of carbon in the system (Taylor & Lloyd 1992; Thompson *et al*. 1996; Kicklighter *et al*. 1999b).

In this study, present-day global NPP was predicted to be $47\,PgC\,y^{-1}$, which is at the low end of the range estimated by others ($48.3–67.6\,PgC\,y^{-1}$, Field *et al*. 1998; $44.4–66.3\,PgC\,y^{-1}$ excluding one outlier, Cramer *et al*. 1999). Our low NPP prediction could be attributed to somewhat low values of short-wave radiation, which

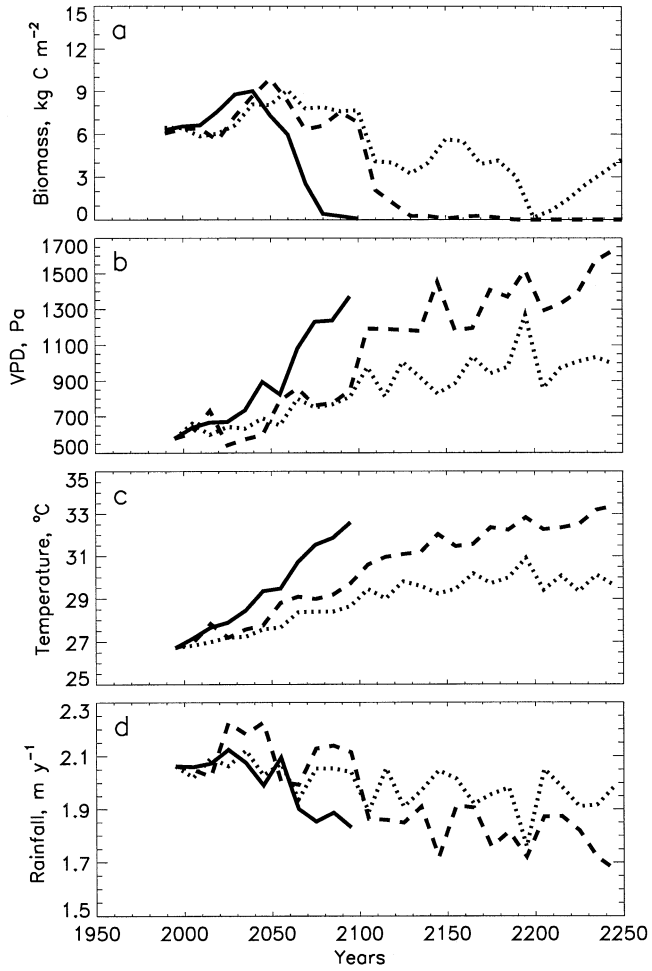

Fig. 8 Predicted vegetation carbon and annual mean climate in a region in northern South America (5.0 °S to 2.5 °N and 67.5–60.0 °W) where the vegetation carbon decreased markedly in response to rapid climate change. (a) Vegetation carbon, (b) vapour pressure deficit (VPD), (c) temperature, and (d) rainfall, with IS92a forcing (solid line), 750 ppm [CO_2] stabilization (dashed line) and 550 ppm [CO_2] stabilization (dotted line). Values shown are decadal means.

were derived using cloud cover in the global observational climatology (Hulme *et al*. 1999). Low NPP values were compensated by relatively high predicted rates of increase in NPP, which increased by about 0.27, 0.20 and 0.16 PgC y^{-1} in the IS92a, 750 and 550 ppm [CO_2] stabilization scenarios, respectively, over the period 1990–2050, when predicted global NEP values were 1–3 PgC y^{-1} (Fig. 4). In Hybrid, canopy photosynthesis responds strongly to increasing CO_2 (Cannell *et al*. 1998) with shifts in N from soil to plants and increases in C:N ratio which may impose less constraint on the CO_2 fertilization response of NPP than in some other models (Rastetter *et al*. 1991; Kicklighter *et al*. 1999b).

The mean residence time of carbon in the Hybrid model was about 25 years in tropical forests and 63 years in boreal forests in 1990 (for the whole system). These values are comparable to those predicted by the Terrestrial Ecosystem and Frankfurt Biosphere Models (see Kicklighter *et al*. 1999b) and those estimated in forest flux studies (Malhi *et al*. 1999; 29 years in a tropical forest and 89 years considered an overestimate for a boreal forest).

In summary, the Hybrid model predicted a current terrestrial carbon sink within the expected range, despite a somewhat low global NPP owing to a large predicted response of NPP to CO_2 fertilization and climate change but a realistic lag between increasing NPP and R_h.

Future development of the global terrestrial carbon sink

The future course of global NEP is determined overwhelmingly by the predicted trajectory of NPP (Thompson *et al*. 1996; Kicklighter *et al*. 1999b). Once the rate of increase in NPP slows, NEP falls; when NPP stabilizes, NEP becomes zero; and if NPP became negative, because of forest dieback for instance, NEP would fall below zero. This pattern of response has been simulated in several studies (McKane *et al*. 1995; Friedlingstein *et al*. 1995; Kicklighter *et al*. 1999b).

Figure 9 compares the time-course of global NPP and NEP predicted in this study with predictions made by Cao & Woodward (1998), Xiao *et al*. (1998) and Sarmiento *et al*. (1995), who are among the few to have published

modelled effects of *transient* climate change and increasing [CO_2] on global terrestrial carbon.

Cao & Woodward (1998) used the same Hadley Centre IS92a projection of [CO_2] and climate as used in the present study (Fig. 9a,b), but predicted a smaller increase in NPP, which could be attributed to a smaller response of canopy photosynthesis to increasing [CO_2] and greater limitations on soil nitrogen supply due to immobilization, as formulated in the DOLY model (Woodward *et al*. 1995; Cramer *et al*. 1999). However, increases in global R_h were lower than in this study, so they predicted a slightly larger NEP up to 2070, but with a similar time trajectory. Notably, their model did not predict forest dieback in the tropics by 2070, possibly because they did not use a weather generator to simulate interannual and seasonal extreme temperatures and VPDs, but also because the temperature response function for dark respiration in DOLY is not fully exponential as it is in the Hybrid (Woodward *et al*. 1995 their fig. 3; see Appendix).

Sarmiento *et al*. (1995) examined the effect of the same IPCC 750 ppm [CO_2] stabilization scenario as used in this study, but predicted less warming (relative to 1990; Fig. 9a,b). They used a simple linear model of GPP as a function of [CO_2], temperature and canopy size, assumed that NPP was 0.8 GPP, and tuned the model to fit deconvolution estimates of NEP since 1850 and to give a current NPP of 60 Pg y^{-1} (cf. 47 PgC y^{-1} in this study). The combination of a high NPP and slow warming resulted in a relatively high predicted NEP. The coupling of GPP and NPP, together with the absence of any water or nutrient constraints on NPP, resulted in a slow decline in NEP after 2050 with no dieback. However, the overall pattern of change in NEP was similar to that predicted in this study with the same 750 ppm [CO_2] stabilization scenario.

Xiao *et al*. (1998) predicted a much slower rate of warming than predicted by HadCM2 in response to a scenario similar to IS92a (using the Integrated Global System Model, developed at the Massachusetts Institute of Technology) and a much slower rate of increase in NPP, using the Terrestrial Ecosystem Model — a highly aggregated model compared with Hybrid (see Heimann *et al*. 1998). TEM predicted a similar global NPP in present-day conditions to Hybrid (Cramer *et al*. 1999), but the much slower continuous increase in NPP resulted in a much slower continuous increase in NEP up to 2100 (Fig. 9). It is likely that, given greater warming, TEM would predict a greater increase in NPP, because warming has a marked positive effect on nitrogen availability in this model. But TEM apparently predicts no stabilization in NPP with increase in [CO_2] above 500–600 ppm, as do the other models in this intercomparison.

Overall, there seems to be a consensus that the current global terrestrial sink will increase during the first half of the next century, in IS92a and 750 and 550 ppm [CO_2] stabilization scenarios. That is, CO_2 fertilization enhancement of NPP will dominate over the temperature enhancement of R_h. Thereafter, the sink must eventually weaken and disappear (as CO_2 fertilization of photosynthesis saturates and warming continues to accelerate R_h) but there is no consensus among the few transient studies conducted to date on when and how rapidly this weakening will occur.

Increase in the high-latitude carbon sink

There are convincing arguments, based on models, direct observations of forest growth and analyses of the atmospheric [CO_2] record, that a large fraction of the current terrestrial carbon sink occurs in high-latitude forests (see Malhi *et al*. 1999). The Hybrid model, driven with HadCM2 climate projections, strongly suggests that the northern forests are a carbon sink now and that this sink will increase over the next century and beyond (Fig. 6). In a more detailed analysis using Hybrid, White *et al*. (2000) suggested that land areas above 50 °N are currently accumulating about 0.4 PgC y^{-1} and that this sink will grow to 0.8–1.0 PgC y^{-1} by 2050 and persist undiminished until 2100, allowing for the effect of fire. About half of the sink could be attributed to [CO_2] fertilization and climate enhancement of NPP and the rest to expansion in the forest area and N deposition. Other recent ecosystem modelling studies support the prediction of a strengthening northern sink, because, at high latitudes, increasing temperatures have a positive effect on NPP, promoting photosynthesis, lengthening the growing season and mineralizing soil nitrogen, amplifying the [CO_2] fertilization effect (Lukewille & Wright 1997; Cao & Woodward 1998; Xiao *et al*. 1998).

At equilibrium, or with increasing [CO_2] alone, a high fraction of the extra carbon would be stored in soils (Malhi *et al*. 1999). But with transient warming, many models, including Hybrid, predict that most or all of the net increase in carbon will be in the trees themselves (Sarmiento *et al*. 1995; Cao & Woodward 1998; Kicklighter *et al*. 1999b; White *et al*. 2000)

Vulnerability of the tropical carbon sink

In this study, tropical forests were predicted to be a carbon sink at present (Fig. 6) in agreement with other modelling studies (Taylor & Lloyd 1992; Cao & Woodward 1998; Kicklighter *et al*. 1999b; see Malhi *et al*. 1999) and some observations (Grace *et al*. 1995; Philips *et al*. 1998; see Malhi *et al*. 1999). However, unlike other modelling studies, Hybrid predicted that substantial forest dieback could occur after 2050 in the IS92a scenario and after 2100 in the 750 ppm [CO_2] stabilization

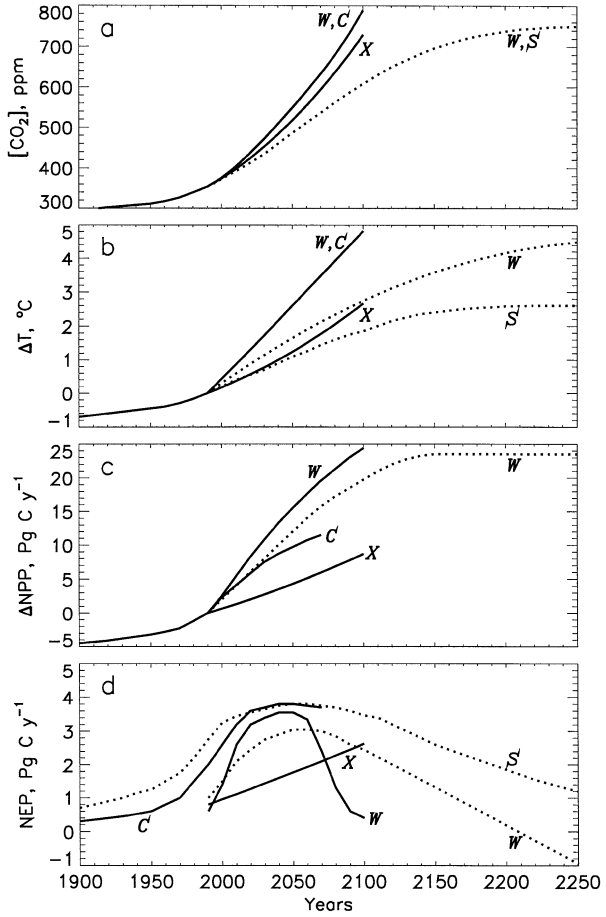

Fig. 9 Results from this study with IS92a forcing and stabilization at 750 ppm compared to other recent studies which combine the effects of transient climate change and increasing CO_2. Solid lines represent IS92a type forcing and dotted lines forcing that would bring about stabilization at 750 ppm CO_2. (a) atmospheric CO_2 concentration, (b) change in global land surface temperature relative to 1990, (c) change in global terrestrial NPP relative to 1990, and (d) global terrestrial NEP. **W**, the results from this study; **C**, Cao & Woodward (1998); **X**, Xiao *et al*. (1998) with their reference scenario (NEP assumed to be 0.8 Pg C y^{-1} in 1990); **S**, Sarmiento *et al*. (1995) with equilibrium warming that would result from the 750 ppm [CO_2] stabilization scenario (Sarmiento *et al*. do not give NPP values). Smooth curves were plotted through the original points to remove large fluctuations in ΔNPP and NEP.

scenario, causing a loss of carbon which could offset the carbon gained at high latitudes, resulting in a rapid loss of the global terrestrial carbon sink (Figs 4c and 6). By contrast, McKane *et al*. (1995) predicted no dieback in the tropics in response to 4 °C warming and [CO_2] doubling over 100 years, nor did Cao & Woodward (1998) in response to the HadCM2 IS92a climate to 2070, nor Xiao *et al*. (1998) in response to about 3 °C warming to 2100. Let us now examine whether our finding might be attributable to the HadCM2 climate predictions and/or to process formulations in the Hybrid model.

The Hadley Centre GCM is consistent with other GCMs in predicting that some tropical land areas will not only warm as much as boreal areas, but will also become drier (Figs 2 and 3). In the HadCM2 transient experiments with an IS92a scenario the areas most prone to longer and more severe dry seasons were in the Amazon basin, southern and western Africa and central and western Australia (Hulme & Viner 1998). The weather generator used in this study simulated interannual and seasonal variability, such that decadal mean increases in temperature of 4 °C were associated with annual excursions of over 6 °C, and decadal mean decreases in rainfall of 10% translated to annual excursions of over 25% with longer dry seasons. It was these large changes in climate that caused forest dieback in the Hybrid model. By contrast, McKane *et al*. (1995) assumed linear warming, while Cao & Woodward (1998) used mean monthly climate values with a monthly timestep. In short, the climate experienced by some tropical forests in this study was more severe in some years than that used in other studies and, by simulating interannual variability, might be regarded as more realistic.

Intuitively, there is reason to suspect that temperature increases of 4–6 °C and decreases in rainfall of 10–25% could be critical for some tropical forests. Although an annual rainfall of only 1.5 m is required to maintain evergreen tropical forest, a drop from say 2.5–1.8 m (see Fig. 8) could result in a shift towards more drought tolerant species (Borchert 1998). Seasonally dry, tall evergreen tropical forests (e.g. in eastern Amazonia) are known to be prone to dieback after successive or severe dry seasons (Borchert 1998; Condit 1998). More generally, it may be argued that any warming or drying in the tropics could be detrimental to evergreen forest growth because metabolic processes in trees and soils are poised so high on response curves, some of which may be exponential (Townsend *et al*. 1992; Neilson & Drapek 1998). A persuasive observation is that, in the tropics, warm years tend to be correlated with low values of the normalized difference vegetation index (NDVI), suggesting that productivity is reduced — the opposite pattern to that observed at high latitudes (Braswell *et al*. 1997).

The changes in temperature and rainfall and associated shifts in VPD that occurred in tropical regions where Hybrid predicted forest dieback, affected many physiological processes in the model. The net result was a decrease in carbon uptake and increase in plant respiration. The critical assumptions were contained in equations for stomatal conductance and maintenance respiration, which are given in the Appendix. Equations A2–A4 predict decreases in stomatal conductance of 70–90% in response to the increases in VPD, temperature

and [CO_2] in the forest dieback areas, drastically lowering canopy photosynthesis and carbon uptake despite the CO_2 fertilization effect. Increased water-use efficiency at elevated [CO_2] was insufficient to compensate for the decrease in rainfall.

Consider, for example, forest dieback in the 2190s at the location illustrated in Fig. 8 in the 550 ppm [CO_2] stabilization scenario. Compared with the 1990s, there had, by then, been increases in decadal mean VPD of 688 Pa, temperature 4.2 °C and [CO_2] 19.7 Pa (Fig. 8). Equations A2–A4 predict a 70% reduction in stomatal conductance, 49% attributable to increased VPD, 27% to increased temperature and 24% to increased [CO_2]. After 2200, more favourable VPDs and temperatures produced only a 47% reduction in stomatal conductance compared to the 1990s and the forest was predicted to regrow (Fig. 8). In the IS92a and 750 ppm [CO_2] stabilization scenarios, continued high temperatures and VPDs prevented regrowth (Fig. 8). Now, the decrease in GPP (gross primary production) could have resulted simply in a proportionate decrease in NPP if it were assumed that respiration was a fixed fraction of GPP (Waring *et al*. 1998). But in Hybrid, maintenance respiration was an exponential function of temperature (eqns A5 and A6), which caused NPP to fall to zero, simulating tree death as temperatures increased and GPP decreased to critical levels.

The Appendix equations offer one valid method of representing stomatal conductance and maintenance respiration which enabled Hybrid to reproduce current ecosystem distribution behaviour reasonably accurately (Cramer & Field 1999; Friend & White 2000). Other ecosystem models achieve similar results using different formulations, incorporating, for instance, the Ball–Berry approach, where stomatal conductance optimizes photosynthesis (Ball *et al*. 1987) or coupling maintenance respiration with assimilate supply (see Cannell & Thornley 2000; Thornley & Cannell 2000). All assume that elevated [CO_2] reduces stomatal conductance, which may not, in fact, be universal (Jarvis *et al*. 1999; Beerling *et al*. 1996). Differences between models become critical when predicting the future, especially in nonoptimal conditions (Cramer & Field 1999) and arise, fundamentally, because we have limited understanding of the physiological mechanisms involved.

In summary, the tropical forest dieback predicted in this study was due in part to the high temperatures and VPDs generated from the GCM output and in part to the formulations of stomatal conductance and maintenance respiration in the Hybrid model. These formulations are plausible, not definitive, and significant forest dieback in the tropics is a plausible consequence of climate change predicted by the Hadley Centre GCM. However, it is only one possible future. Many more studies of this kind are required, testing different DGVM formulations.

Conclusion

This study reinforces previous evidence that there is currently a carbon sink in both the northern and tropical forests. It also suggests that the northern sink will continue to increase for at least a century with IS92a emissions or 750 and 550 ppm [CO_2] stabilization. However, unlike previous studies, the climate scenario and DGVM used here predict that the IS92a emissions scenario might carry a risk of catastrophic collapse of some tropical forest ecosystems within the next 100 years. Stabilizing [CO_2] at 750 ppm would postpone this collapse by about 100 y, but it would still be substantial. Stabilizing [CO_2] at 550 ppm carries much less risk of forest dieback in the tropics and if it did occur the climate might be favourable enough for recovery. Clearly, avoiding tropical forest dieback is important for reasons extending far beyond the issue of maintaining the terrestrial carbon sink. Any fall in potential primary productivity in the tropics is likely to have significant effects on biodiversity, agricultural production and the well-being of millions of people.

Acknowledgements

We are grateful to Tim Lenton for helpful comments on this paper. This work was funded by the UK Department of Environment, Transport and Regions under contract number EPG1/1/64.

References

Ball JT, Woodrow IE, Berry JA (1987) A model predicting stomatal conductance and its contribution to the control of photosynthesis under different environmental conditions. In: *Progress in Photosynthesis Research*, Vol. IV. *Proceedings of the Viith International Congress on Photosynthesis* (ed. Biggin I), pp. 221–224. Nijhoff, Dordrecht.

Beerling DJ, Heath J, Woodward FI, Mansfield TA (1996) Drought–CO_2 interactions in trees: observations and mechanisms. *New Phytologist*, **134,** 235–242.

Borchert R (1998) Responses of tropical trees to rainfall seasonality and its long-term changes. *Climatic Change*, **39,** 381–393.

Braswell BH, Schimel DS, Linder E, Moore III B (1997) the response of global terrestrial ecosystems to inter-annual temperature variability. *Science*, **278,** 870–872.

Bruno M, Joos F (1997) Terrestrial carbon storage during the past 200 years: a Monte Carlo analysis of CO_2 data from ice-core and atmospheric measurements. *Global Biogeochemical Cycles*, **11,** 111–124.

Cannell MGR, Thornley JHM (2000) Modelling the components of plant respiration. I: some guiding principles. *Annals of Botany*, **85**, 45–54.

Cannell MGR, Thornley JHM, Mobbs DC, Friend AD (1998) UK conifer forests may be growing faster in response to increased N deposition, atmospheric CO_2 and temperature. *Forestry*, **71,** 277–296.

Cao M, Woodward FI (1998) Dynamic responses of terrestrial ecosystem carbon cycling to global climate change. *Nature*, **393,** 249–252.

Chen WJ, Black TA, Yang PC *et al.* (1999) Effects of climatic variability on the annual carbon sequestration by a boreal forest. *Global Change Biology*, **5,** 41–53.

Ciret C, Henderson-Sellers A (1997) Sensitivity of global vegetation models to present-day climate simulated by global climate models. *Global Biogeochemical Cycles*, **11,** 415–434.

Cleveland CC, Townsend AR, Schimel DS *et al.* (1999) Global patterns of terrestrial biological nitrogen (N_2) fixation in natural ecosystems. *Global Biogeochemical Cycles*, **13,** 623–645.

Collatz GJ, Ball JT, Grivet C, Berry JA (1991) Physiological and environmental regulation of stomatal conductance, photosynthesis and transpiration: a model that includes a laminar boundary layer. *Agricultural and Forest Meteorology*, **54,** 107–136.

Comins HN, Mcmurtrie RE (1993) Long-term response of nutrient-limited forests to CO_2 enrichment. *Ecological Applications*, **3,** 666–682.

Condit R (1998) Ecological implications of changes in drought patterns: shifts in forest composition in Panama. *Climatic Change*, **39,** 413–427.

Cramer W, Field CB (eds) (1999) The Potsdam NPP model intercomparison. *Global Change Biology*, **5** (Suppl. 1), 76pp.

Cramer W, Kicklighter DW, Bondeau A *et al.*(1999) Comparing global models of terrestrial net primary productivity (NPP): overview and key results. *Global Change Biology*, **5** (Suppl. 1), 1–15.

Farquhar GD, von Caemmerer S (1982) Modelling of photosynthetic response to environmental conditions. In: *Physiological Plant Ecology II. Water Relations and Carbon Assimilation* (eds Lange O *et al.*), pp. 549–587. Springer, Berlin.

Field CB, Behrenfeld MJ, Randerson JT, Falkowski P (1998) Primary production of the biosphere: integrating terrestrial and oceanic components. *Science*, **281,** 237–240.

Foley JA, Prentice IC, Ramankutty N, Levis S, Pollard D, Sitch S, Haxeltine A (1996) An integrated biosphere model of land surface processes, terrestrial carbon balance and vegetation dynamics. *Global Biogeochemical Cycles*, **10,** 603–628.

Friedlingstein P, Fung I, Holland E, John J, Brasseur G, Erickson D, Schimel D (1995) On the contribution of CO2 fertilization to the missing biospheric sink. *Global Biogeochemical Cycles*, **9,** 541–556.

Friend AD (1995) PGEN: an integrated model of leaf photosynthesis, transpiration and conductance. *Ecological Modelling*, **77,** 233–255.

Friend AD (1998) Parameterisation of a global daily weather generator for terrestrial ecosystem modelling. *Ecological Modelling*, **109,** 121–140.

Friend AD, White A (2000) Evaluation and analysis of a dynamic terrestrial ecosystem model under pre-industrial conditions at the global scale. *Global Biogeochemical Cycles*, in press.

Friend AD, Stevens AK, Knox RG, Cannell MGR (1997) A process-based, biogeochemical, terrestrial biosphere model of ecosystem dynamics (Hybrid v3.0). *Ecological Modelling*, **95,** 249–287.

Grace J, Lloyd J, Mcintyre J *et al.*(1995) Carbon dioxide uptake by an undisturbed tropical rain forest in southwest Amazonia. *Science*, **270,** 778–780.

Heimann M, Esser G, Haxeltine A *et al.* (1998) Evaluation of terrestrial carbon cycle models through simulations of the seasonal cycle of atmospheric CO_2: first results of a model intercomparison study. *Global Biogeochemical Cycles*, **12,** 1–24.

Holland EA, Braswell BH, Lamarque JF *et al.* (1997) Variations in the predicted spatial distribution of atmospheric nitrogen deposition and their impact on carbon uptake by terrestrial ecosystems. *Journal of Geophysical Research*, **102,** 15,849–15,866.

Houghton RA, Davidson EA, Woodwell GM (1998) Missing sinks, feedbacks and understanding the role of terrestrial ecosystems in the global carbon balance. *Global Biogeochemical Cycles*, **12,** 25–34.

Hudson RJM, Gherini SA, Goldstein RA (1994) Modeling the global carbon cycle: nitrogen fertilization of the terrestrial biosphere and the 'missing' sink. *Global Biogeochemical Cycles*, **8,** 307–333.

Hulme M, Viner D (1998) A climate change scenario for the tropics. *Climatic Change*, **39,** 145–176.

Hulme M, Mitchell J, Ingram M, Johns T, New M, Viner D (1999) Climate change scenarios for global impacts studies. *Global Environmental Change*, **9,** S3–S19.

Hurtt GC, Moorcroft PR, Pacala SW, Levin SA (1998) Terrestrial models and global change: challenges for the future. *Global Change Biology*, **4,** 581–590.

Jarvis PG (1976) The interpretation of the variation in leaf water potential and stomatal conductance found in canopies in the field. *Philosophical Transactions of the Royal Society of London B*, **273,** 593–610.

Jarvis AJ, Mansfield TA, Davies WJ (1999) Stomatal behaviour, photosynthesis and transpiration under rising CO_2. *Plant, Cell and Environment*, **22,** 639–648.

Johns TC, Carnell RE, Crossley JF *et al.*(1997) The second Hadley Centre coupled ocean-atmosphere GCM: model description, spinup and validation. *Climate Dynamics*, **13,** 103–134.

Kaduk J, Heimann M (1994) The climate sensitivity of the Osnabruck Biosphere Model on the ENSO timescale. *Ecological Modelling*, **75/76,** 239–256.

Kattenberg A, Giorgi F, Grassl H *et al.* (1996) Climate models – projection of future climates. In: *Climate Change. The Science of Climate Change. Contribution to Working Group I to the Second Assessment Report of the IPCC* (eds Houghton JT *et al.*), pp. 285–357. Cambridge University Press, Cambridge.

Keeling CD, Whorf TP, Wahlen M, van der Pilcht J (1995) Interannual extremes in the rate of rise of atmospheric carbon dioxide since 1980. *Nature*, **375,** 666–670.

Kicklighter DW, Bondeau A, Schloss AL *et al.* (1999a) Comparing global models of terrestrial net primary productivity (NPP): global pattern and differentiation by major biomes. *Global Change Biology*, **5,** 16–24.

Kicklighter DW, Bruno M, Donges S *et al.* (1999b) A first-order analysis of the potential role of CO_2 fertilization to affect the global carbon budget: a comparison of four terrestrial biosphere models. *Tellus*, **51B,** 343–366.

Kindermann J, Gurth W, Kohlmaier GH (1996) Interannual variation of carbon exchange fluxes in terrestrial ecosystems. *Global Biogeochemical Cycles*, **10,** 737–755.

Körner C (1994) Leaf diffusive conductances in the major vegetation types of the globe. In: *Ecophysiology of*

Photosynthesis (eds Schulze E-D, Caldwell MM), pp. 463–489. Springer, Berlin.

Lean J, Brunton CB, Nobre CA, Rowntree PR (1996) The simulated impact of Amazonian deforestation on climate using measured ABRACOS vegetation characteristics. In: *Amazonian Deforestation and Climate* (eds Gash JHC *et al.*), pp. 549–576. Wiley, Chichester.

Lenton T (2000) Land and ocean carbon cycle feedback effects on global warming in a simple earth system model. *Tellus*, **52B**, 5, in press.

Lloyd J, Farquhar GD (1996) The CO_2 dependence of photosynthesis, plant growth responses to elevated CO_2 concentrations and their interaction with soil nutrient status. General principles and forest ecosystems. *Functional Ecology*, **10,** 4–32.

Lukewille A, Wright RF (1997) Experimentally increased soil temperature causes release of nitrogen at a boreal forest catchment in southern Norway. *Global Change Biology*, **3,** 13–21.

Malhi Y, Baldocchi DD, Jarvis PJ (1999) The carbon balance of tropical, temperate and boreal forests. *Plant, Cell and Environment*, **22,** 715–740.

Mcguire AD, Melillo JM, Kicklighter DW *et al.* (1997) Equilibrium responses of global net primary production and carbon storage to doubled atmospheric carbon dioxide: sensitivity to changes in vegetation nitrogen *Concentration. Global Biogeochemical Cycles*, **11,** 173–189.

McKane RB, Rastetter EB, Melillo JM, Shaver GR, Hopkinson CS, Fernandes DN (1995) Effects of global change on carbon storage in tropical forests of South America. *Global Biogeochemical Cycles*, **9,** 329–350.

Mitchell JFB, John TC, Gregory JM, Tett SFB (1995) Climate response to increasing levels of greenhouse gases and sulphate aerosols. *Nature*, **376,** 501–504.

Nadelhoffer KJ, Emmett BA, Gundersen P *et al.* (1999) Nitrogen deposition makes a minor contribution to carbon sequestration in temperate forests. *Nature*, **398,** 145–148.

Neilson R, Drapek RJ (1998) Potentially complex biosphere responses to transient global warming. *Global Change Biology*, **4,** 505–521.

Neilson RP, Running SW (1996) Global dynamic vegetation modeling: coupling biogeochemisry and biogeography models. In: *Global Change and Terrestrial Ecosystems* (eds Walker B, Steffen W), pp. 451–465. Cambridge University Press, Cambridge.

Neilson RP, Prentice IC, Kittel T, Viner D (1998) Simulated changes in vegetation distribution under global warming. In: *The Regional Impacts of Climate Change: an Assessment of Vulnerability, a Special Report of IPCC WG II* (eds Watson RT *et al.*), pp. 440–456. Intergovernmental Panel on Climate Change/ Cambridge University Press, Cambridge.

New MG, Hulme M, Jones PD (1999) Representing twentieth century space-time climate variability. Part 1: development of a 1961–90 mean monthly terrestrial climatology. *Journal of Climate*, **12,** 829–856.

Parry ML, Carter TR, Hulme M (1996) What is a dangerous climate change? *Global Environmental Change*, **6,** 1–6.

Parton WJ, Scurlock JMO, Ojima DS *et al.* (1993) Observations and modelling of biomass and soil organic matter dynamics for the grassland biome worldwide. *Global Biogeochemical Cycles*, **7,** 785–809.

Parton WJ, Scurlock JMO, Ojima DS, Schimel DS, Hall DO, Scopegram members (1995) Impact of climate change on grassland production and soil carbon worldwide. *Global Change Biology*, **1,** 13–22.

Philips OL, Malhi Y, Higuchi N *et al.* (1998) Changes in the carbon balance of tropical forests: evidence from long-term plots. *Science*, **282,** 439–441.

Post WM, Emanuel WR, Zinke PJ, Stangenberger AG (1982) Soil Carbon pools and world life zones. *Nature*, **298,** 156–159.

Post WM, King AW, Wullschleger SD (1997) Historical variations in terrestrial biospheric carbon storage. *Global Biogeochemical Cycles*, **11,** 99–109.

Potter CS, Klooster SA (1999) Detecting a terrestrial biosphere sink for carbon dioxide: inter-annual ecosystem modeling for the mid-1980s. *Climatic Change*, **42,** 489–503.

Rastetter EB, Ryan MG, Shaver GR *et al.* (1991) A general biogeochemical model describing the responses of the C and N cycles in terrestrial ecosystems to changes in CO_2, climate and N deposition. *Tree Physiology*, **9,** 101–126.

Richardson CW, Wright DA (1984) Wgen: a Model for Generating Daily Weather Variables. U.S. Department of Agriculture, Agricultural Research Service, Washington, DC.

Ryan MG (1990) Growth and maintenance respiration in stems of *Pinus contorta* and *Picea engelmannii*. *Canadian Journal of Forest Research*, **20,** 48–57.

Ryan MG (1991) A simple method for estimating gross carbon budgets for vegetation in forest ecosystems. *Tree Physiology*, **9,** 255–266.

Sarmiento JL, Le Quéré C, Pacala SW (1995) Limiting future atmospheric carbon dioxide. *Global Biogeochemical Cycles*, **9,** 121–137.

Schimel DS, Braswell BH, Mckeown R, Ojima DS, Parton WJ, Pulliam W (1996) Climate and nitrogen controls on the geography and timescales of terrestrial biogeochemical cycling. *Global Biogeochemical Cycles*, **10,** 677–692.

Schimel D, Enting IG, Heimann M *et al.* (1995) CO_2 and the carbon cycle. In: *Climate Change 1994. Radiative Forcing of Climate Change and Evaluation of the IPCC IS92 Emission Scenarios* (eds Houghton JT *et al.*), pp. 35–71. Cambridge University Press, Cambridge.

Schimel D, Grubb M, Joos F *et al.* (1997b) *Stabilization of Atmospheric Greenhouse Gases: Physical, Biological and Socio-Economic Implications.* Technical Paper III. Intergovernmental Panel on Climate Change/WMO, Geneva.

Schimel DS, Emanuel W, Rizzo B *et al*. (1997a) Continental scale variability in ecosystem processes: models, data and the role of disturbance. *Ecological Monographs*, **67,** 251–271.

Shugart HH (1984) *Theory of Forest Dynamics*. Springer, Berlin, 278pp.

Stewart JB (1988) Modelling surface conductance of pine forest. *Agricultural and Forest Meteorology*, **43,** 19–35.

Taylor JA, Lloyd J (1992) Sources and sinks of atmospheric CO_2. *Australian Journal of Botany*, **40,** 407–418.

Thompson MV, Randerson JT, Malstrom CM, Field CB (1996) Change in net primary production and heterotrophic respiration: how much is necessary to sustain the terrestrial carbon sink? *Global Biogeochemical Cycles*, **10,** 711–726.

Thornley JHM, Cannell MGR (2000) Modelling the components of plant respiration II. Representation and realism. *Annals of Botany*, **85**, 55–67.

Townsend AR, Braswell BH, Holland EA, Penner JE (1996) Spatial and temporal patterns in terrestrial carbon storage due

to deposition of fossil fuel nitrogen. *Ecological Applications*, **6,** 806–814.
Townsend AR, Vitousek PM, Holland EA (1992) Tropical soils could dominate the short-term carbon cycle feedbacks to increased global temperatures. *Climatic Change*, **22,** 293–303.
Vemap members (1995) Vegetation/ecosystem modeling and analysis project: comparing biogeography and biogeochemical models in a continental-scale study of terrestrial ecosystem responses to climate change and CO_2 doubling. *Global Biogeochemical Cycles*, **9,** 407–437.
Wang YP, Polglase PJ (1995) Carbon balance in the tundra, boreal forest and humid tropical forest during climate change: scaling up from leaf physiology and soil carbon dynamics. *Plant, Cell and Environment*, **18,** 1226–1244.
Waring RH, Landsberg JJ, Williams M (1998) Net production of forests: a constant fraction of gross primary production. *Tree Physiology*, **18,** 129–134.
White A, Cannell MGR, Friend AD (1999) Climate change impacts on ecosystems and the terrestrial carbon sink: a new assessment. *Global Environmental Change*, **9,** S21–S30.
White A, Cannell MGR, Friend AD (2000) The high-latitude terrestrial carbon sink: a model analysis. *Global Change Biology*, **6,** 227–247.
Woodward FI, Smith TM, Emanuel WR (1995) A global land primary productivity and phytogeography model. *Global Biogeochemical Cycles*, **4,** 471–490.
Xiao X, Kicklighter DW, Melillo JM, Mcguire AD, Stone PH, Sokolov AP (1997) Linking a global terrestrial biogeochemical model with a 2-dimensional climate model: implications for global carbon budget. *Tellus*, **49B,** 18–37.
Xiao X, Melillo JM, Kicklighter DW *et al.* (1998) Transient climate change and net ecosystem production of the terrestrial biosphere. *Global Biogeochemical Cycles*, **12,** 345–360.

Appendix

The model Hybrid v4.1 predicts forest dieback in some regions, which could be traced to a decrease in gross primary production, as a result of stomatal closure, while maintenance respiration remained relatively constant or increased.

In the model, stomatal conductance, g, is calculated using the approach of Jarvis/Stewart (Jarvis 1976; Stewart 1988) by multiplying a hypothetical maximum conductance, g_{max}, by functions of solar radiation, δ_{rad}, specific humidity deficit, δ_{dq}, air temperature, δ_T, soil water potential, δ_{sw}, and above-canopy CO_2 concentration, δ_{CO2}:

$$g = g_{max} \cdot \delta_{rad} \cdot \delta_{dq} \cdot \delta_T \cdot \delta_{sw} \cdot \delta_{CO_2}, \qquad (A1)$$

where g_{max} is calculated from the amount of foliage nitrogen bound in rubisco and scaled to give the appropriate relationship between g_{max} and net photosynthesis, A_{max}, as detail by Körner (1994) (see Friend *et al*. 1997). For the tropical regions where dieback was predicted to occur (Fig. 8), the factors relating to solar radiation and soil water potential were relatively constant during all simulations. The other factors are detailed below. Linear stomatal closing was assumed with specific humidity deficit, such that

$$\delta_{dq} = \begin{cases} 1 - 1.219 \cdot \dfrac{\theta_d}{R \cdot T} & \text{if } \dfrac{\theta_d}{R \cdot T} \le 0.6277 \\ 0.2348 & \text{if } \dfrac{\theta_d}{R \cdot T} > 0.6277 \end{cases}, \qquad (A2)$$

where θ_d is the vapour pressure deficit (VPD) of the atmosphere (Pa), R is the gas constant (= 8.3144 J K^{-1} mol^{-1}) and T is air temperature (K). At standard temperature and pressure the minimum value is reached with a VPD of 1530 Pa.

For air temperatures below 0 or above 40 °C, $\delta_T = 0$, otherwise

$$\delta_T = \frac{(T \cdot (40 - T))^{1.18}}{(18.35 \cdot (40 - 18.35))^{1.18}}, \qquad (A3)$$

where T is the air temperature (°C). This factor displays a super-linear relationship between 0 and 40 °C with a maximum of 1 at 18.35 °C.

A linear closing response with increasing CO_2 was assumed whereby

$$\delta_{CO_2} = \begin{cases} 1 - 0.00833 \cdot co & \text{if } co \le 80 \\ 0.333 & \text{if } co > 80 \end{cases}, \qquad (A4)$$

where co is the atmospheric CO_2 partial pressure (Pa) and a minimum is reached at 80 Pa.

Daytime and night-time maintenance respiration was calculated for fine root, sapwood (or support structure in herbaceous plant) and foliage components separately. (Foliage had a night-time component only as the daytime component is implicit in photorespiration.) The mean night-time foliage maintenance respiration rate, $F_{f,n}$ was assumed to be a linear function of foliage nitrogen content and an exponential function of air temperature (after Ryan 1991; Friend *et al*. 1997):

$$F_{f,n} = \eta_{f,n} \cdot N_f \cdot e^{-6595/T_n}. \qquad (A5)$$

here, subscript f denotes foliage and n denotes night-time, $\eta_{f,n}$ is a constant estimated from Ryan (1991) to be 42.6×10^3 kg C kg N^{-1} s^{-1}, and T_n denotes night-time air temperature (K).

Mean fine root maintenance respiration over each 24-h period, F_r, was calculated from fine root nitrogen content N_r, and mean 24 h soil temperature, using the same formulation as equation (A5).

Sapwood and grass support tissue respiration rates were calculated for daytime, $F_{w,d}$, and night-time, $F_{w,n}$, assuming a linear relationship with living carbon mass, C_v, and a exponential relationship with air temperature (after Ryan 1990; Friend *et al*. 1997):

$$F_{w,d/n} = \eta_w \cdot C_v \cdot e^{-6595/T_{d/n}} \qquad (A6)$$

The constant η_w was estimated from the measurements of Ryan (1990) to be 83.14 kg C kg C^{-1} s^{-1}.

If carbon and nitrogen pools remained relatively constant, total plant maintenance respirational depended critically on air temperature. In Hybrid, maintenance respiration is not coupled directly to photosynthesis, and therefore the fraction of assimilates used in respiration could exceed 0.6, especially as trees died at high temperatures (cf. Waring *et al*. 1998; Cannell & Thornley 2000).